Yang *et al. Biomarker Research* (2026) 14:35
https://doi.org/10.1186/s40364-026-00896-1

Biomarker Research

CORRESPONDENCE Open Access

Proteome-based molecular subtyping and therapeutic target prediction in cervical cancer

Tianying Yang[1†], Luopei Guo[1†], Danyang Liu[2†], Keqin Hua[1*] and Chunbo Li[1*]

Abstract

Cervical cancer (CC) represents a leading malignant threat to women's health globally. Patients with advanced-stage CC frequently encounter limited therapeutic efficacy and prominent drug resistance, highlighting the urgent need for molecular-driven precision treatment strategies. Herein, we developed a proteomics-based molecular classification for CC. A total of 198 CC patients were classified into four distinct molecular subtypes: CC-I ($n=55$), CC-II ($n=32$), CC-III ($n=43$), and CC-IV ($n=68$). This classification system was further validated in an independent cohort, confirming its clinical reliability. Survival analysis indicated significant prognostic differences among the four subtypes (log-rank test, $p<0.001$). Functional analysis revealed distinct molecular characteristics: CC-I and CC-IV were characterized by enrichment of immune-related pathways, while CC-II and CC-III displayed upregulated metabolism-associated pathways. Notably, CC-IV overexpressed pathways associated with cell cycle regulation, p53 signaling, and DNA repair, potentially contributing to its aggressive phenotype. Meanwhile, CC-I and CC-IV had higher immune scores and were enriched with T cells and B cells, suggesting potential favorable responsiveness to immunotherapies. Focusing on the CC-IV, we observed that high CDK4/6 expression was correlated with poor clinical outcomes. Patient-derived organoid (PDO) models confirmed that CDK4/6 inhibitor (palbociclib) had significant growth-inhibitory effects on CC patients with high CDK4/6 expression. In conclusion, this study established the first validated proteome-based molecular subtyping system for CC, and identified actionable therapeutic targets, and provided a robust foundation for personalized treatment strategies in CC.

Keywords Cervical cancer, Proteomics, Molecular subtyping, Therapeutic targets, CDK4/6 inhibitors

To the editor

Cervical cancer (CC) severely threatens women's health globally, with over 600,000 new cases and approximately 340,000 deaths annually and rising incidence/mortality in developing countries [1]. However, current treatments for CC are far from satisfactory. The efficacy of targeted drugs or immunotherapies remains limited, highlighting an urgent need to break through the current therapeutic bottleneck [2]. Accurate molecular subtyping is critical for CC. Extensive efforts have been made using genomic and transcriptomic data, but with limited impact on clinical decisions [3]. Proteins provide insight into the

†Tianying Yang, Luopei Guo and Danyang Liu have contributed equally to this work.

*Correspondence:
Keqin Hua
huakeqinjiaoshou@126.com
Chunbo Li
lichunbo142@126.com
[1]Department of Obstetrics and Gynecology, Obstetrics & Gynecology Hospital of Fudan University, Shanghai Key Lab of Reproduction and Development, Shanghai Key Lab of Female Reproductive Endocrine Related Diseases, Shanghai 200433, China
[2]Department of Pathology, Obstetrics & Gynecology Hospital of Fudan University, Shanghai Key Lab of Reproduction and Development, Shanghai Key Lab of Female Reproductive Endocrine Related Diseases, Shanghai 200433, China

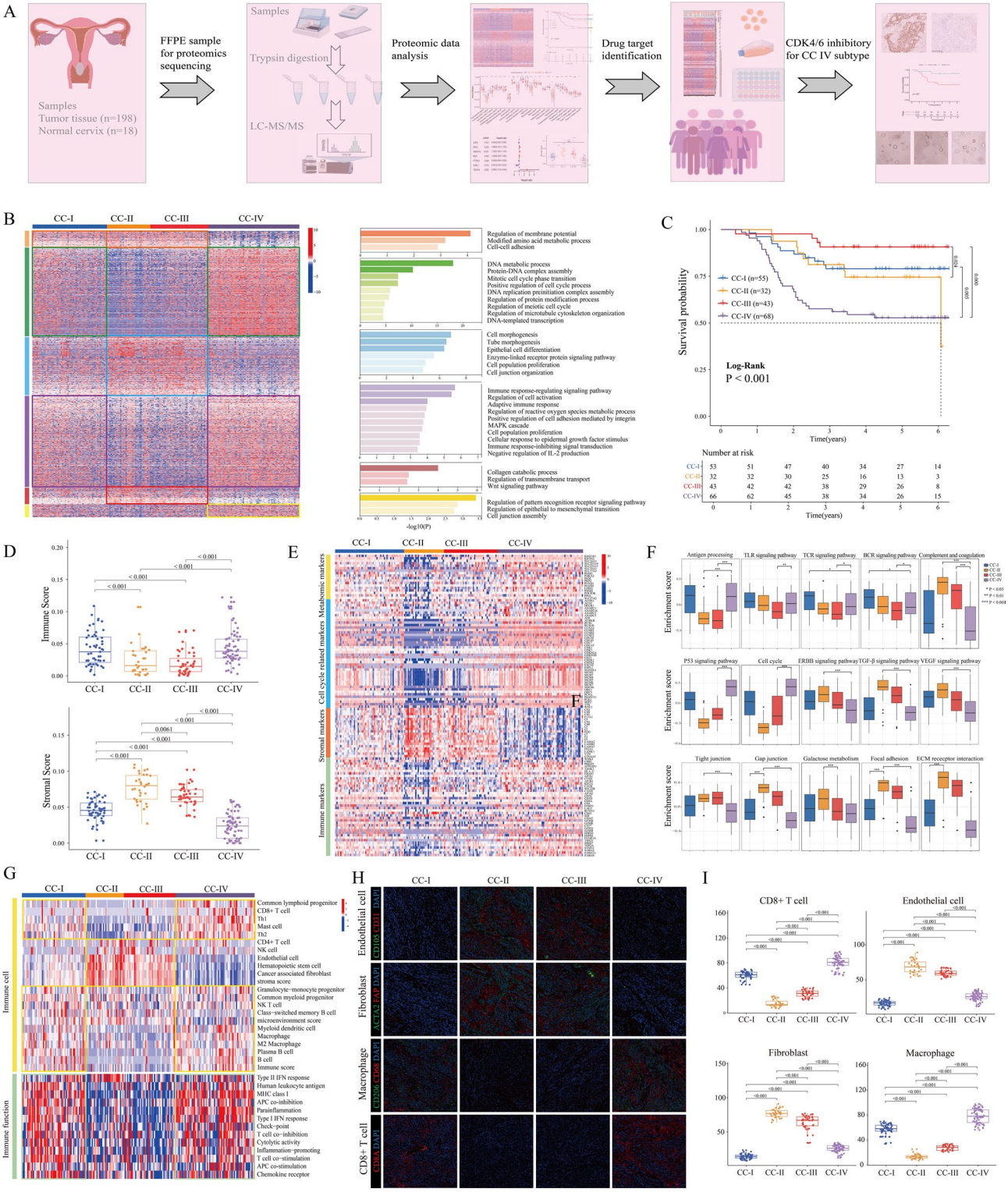

Fig. 1 (See legend on next page.)

disease at the protein level. To date, there is still a lack of a well-validated CC classification system based on proteomics [4].

We performed comprehensive proteomic analysis to define CC molecular subtypes using a discovery cohort (198 samples) (Fig. 1A and Supplemental Table. S1) and a validate cohort (129 samples) [5]. Consensus clustering

(See figure on previous page.)

Fig. 1 Proteome-based molecular subtyping of cervical cancer (CC). (**A**) schematic illustration of the workflow, including tissue sample punching, sample information annotation, batch design, and subsequent proteomic data analysis. (**B**) heatmap visualizing the expression profiles of significantly differentially expressed proteins (DEPs) among the four CC subtypes. Six clusters of subtype-specific DEPs are highlighted with the top enriched pathways (analyzed by Metascape) labeled alongside the corresponding proteins in each cluster. (**C**) cancer-specific overall survival (OS) curves of the four subtypes, depicting changes in survival probability (y-axis) over time (x-axis). P-value is calculated by two-sided log rank test. (**D**) comparison of immune score and stromal score among the four subtypes. Boxplots are constructed with the box representing the interquartile range (IQR, 25th to 75th percentiles), the horizontal line inside the box indicating the median, and whiskers extending to data points within 1.5× IQR. (***$p < 0.001$, **$p < 0.01$). (**E**) heatmap illustrating marker proteins across the four subtypes, with annotations of metabolism, cell cycle, immune/stromal signatures derived from global proteomics data. (**F**) comparison of significantly enriched functions among the four subtypes. Boxplot construction follows the criteria described in (**D**). (***$p < 0.001$, **$p < 0.01$). (**G**) heatmap illustrating cell-type compositions and pathway activities across the four subtypes. The upper section presents immune/stromal signatures inferred by xCell; the lower section shows single-sample gene set enrichment analysis (ssGSEA) scores of upregulated biological pathways in the four subtypes, based on global proteomics data. (**H**) multilabel immunofluorescence (MIF) staining of CC samples from the four CC subtypes. Antibodies against CD8 (red), CD206 (green), CD68 (red), ACTA2 (green), FAP (red), CD31 (red) and CD105 (green) are used to quantify cell types in tissue sample of the four subtypes. Scale bars, 50 mm. (**I**) comparison of cell-type abundance in CC samples across the four CC subtypes based on MIF profiling. Each dot in boxplot represents one CC specimen. Boxplot construction follows the criteria described in (**D**). (***$p < 0.001$, **$p < 0.01$)

of 198 samples based on 486 survival-related proteins (Fig. 1A–B) identified four subtypes (Fig. 1B and Supplemental Table. 1). Survival analysis revealed a significant association between these proteomic subtypes and prognosis (Fig. 1C). CC-IV was characterized by advanced clinical stage, and a higher proportion of squamous cell carcinoma (Fig. 2A–B). The four subtypes were further verified in an independent cohort [4], confirming the reliability of the classification (Figure. S1A-B and Figure. S4).

Subtype-specific functional analysis revealed distinct differences among the four subtypes (Fig. 1D–E). Gene Set Variation Analysis showed that immune-related pathways were highly enriched in CC-I and CC-IV; metabolism-related pathways in CC-II and CC-III; and cell cycle, DNA repair, and p53 pathways specifically in CC-IV (Figure. S5A-B). We then explored the functional differences between CC-I and CC-IV (Figure. S6A-C and Supplemental Table. S3). Up-regulated proteins in CC-IV were associated with mismatch repair, p53 signaling, and cell cycle, whereas cell adhesion molecules, focal adhesion, and apical junction were highly enriched in CC-I (Figure. S6B-C). CC-III and CC-IV represented two distinct subtypes (Fig. 1D–E and Supplemental Table. S4). Comparative analysis (Figure. S6D-F and Supplemental Table. S5) showed that CC-III was associated with high enrichment of metabolism-related pathways, ECM receptor interaction, and focal adhesion, while CC-IV was enriched in cell cycle, and immune-related pathway signaling pathways (Fig. 1E–F). Notably, CC-IV also exhibited high enrichment of P53 signaling, hypoxia, and angiogenesis (Figure. S6D-F). Screening of transcription factors (TFs) activity can enhance our understanding of CC heterogeneity. We evaluated inferred TFs activities and their targets at the proteomic level and identified the master TFs in each subtype: ZEB1/2 dominated in CC-III, while E2F8, TFDP1, and MCM2 were dominant in CC-IV (Figure. S7A-B). Functional analysis based on TFs also revealed consistent characteristics with proteomic profiles (Figure. S7C).

To systematically characterize the tumor microenvironment (TME) across the four subtypes, we analyzed the distribution of major tumor-infiltrating immune cells. CC-I and CC-IV were associated with high levels of CD4+T cell, Th1 cells, Mast cell and B cells (Fig. 1G). ssGSEA showed that CC-I and CC-IV had high enrichment of immune-related signaling pathways (Fig. 1G). The expressions of immune molecules were up-regulated in CC-I and CC-IV (Figure. S8A-B). The infiltration of immune and mesenchymal cells was validated by multilabel immuno-fluorescence (MIF) staining. CC-I and CC-IV subtypes were enriched with macrophages and CD8 T cells, while CC-II and CC-III subtypes were enriched with endothelial cells and fibroblasts (Fig. 1H–I). We thus hypothesized that both CC-I and CC-IV have an active TME and may benefit from immunotherapy, which may be attributed to immune dysfunction driven by T-cell exhaustion, immunosuppressive cell dominance, and tumor cell-intrinsic resistance, forming a non-functional "inflamed" TME [6, 7].

Focusing on the CC-IV, we investigated the therapeutic potential of targeting the cell cycle. First, we observed that a series of cell cycle-related proteins were highly expressed in CC-IV (Fig. 2A). Among these, high expressions of CDK4 and CDK6 were associated with poor prognosis (Fig. 2B). TCGA confirmed that high CDK6 correlated with unfavorable survival (Fig. 2C). Immunohistochemical analysis revealed that high CDK4 and CDK6 expressions were associated with poor OS (Fig. 2D). We then established patient-derived organoids (PDOs) from fresh tumor tissues with high or low CDK4/6 expression (Fig. 2E). Compared with the CDK4/6^{low} PDOs, palbociclib significantly inhibited the growth of CDK4/6^{high} PDOs at a concentration of 5uM (Fig. 2F). Drug sensitivity analysis showed that the half maximal inhibitory concentration (IC50) of palbociclib was higher in CDK4/6^{low} PDOs (21.35 uM) than in CDK4/6^{high} PDOs (IC50 = 7.47 uM) (Fig. 2G), suggesting that CC with high cell cycle activity may be sensitive to palbociclib.

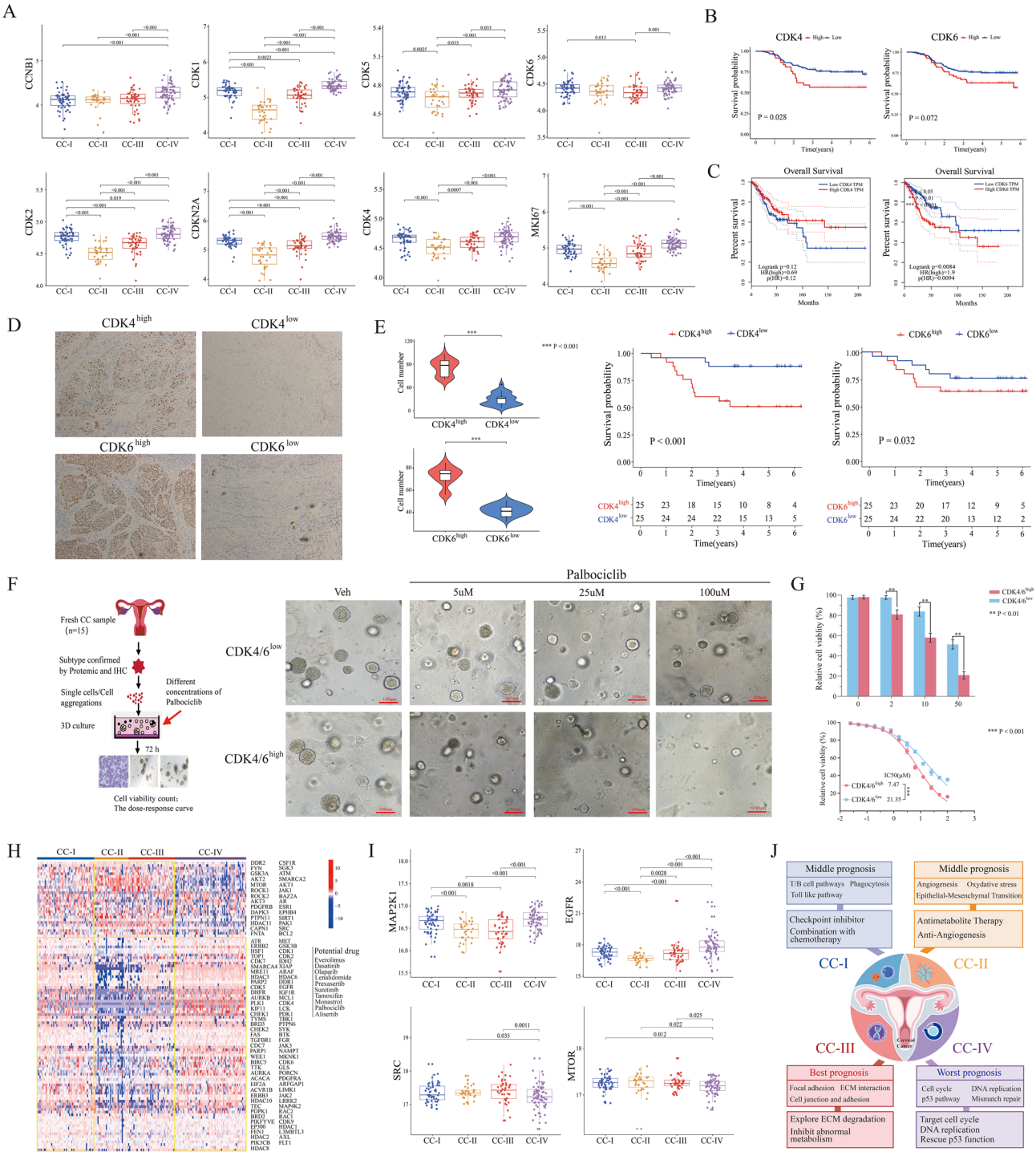

Fig. 2 (See legend on next page.)

In addition, we identified other potential subtype-specific therapeutic targets by screening solid tumor drug targets from the DrugBank database [5]. 119 quantifiable drug targets with significant abundance differences among the four subtypes were identified (Fig. 2H and Supplemental Table. S6). For example, DNA damage repair-related targets were highly expression in CC-IV, suggesting the potential value of Olaparib and Prexasertib [8, 9]. The high kinase activity of EGFR and MAP2K1 in CC-IV, suggested that combination therapy targeting EGFR and mTOR pathways may be a more effective for CC-IV (Fig. 2I). We also identified ten potential targets

(See figure on previous page.)

Fig. 2 Potential drug targets across the four subtypes. (**A**) comparison of cell cycle-related marker protein expression among the four subtypes. (**B**) association of CDK4 and CDK6 expression with patient survival in the proteomic cohort. P-value is calculated by two-sided log rank test. (**C**) association of CDK4 and CDK6 expression with patient survival in the cancer Genome Atlas (TCGA) cohort. P-value is calculated by two-sided log rank test. (**D**) immunohistochemical analysis of CDK4 and CDK6 expression and its correlation with patient prognosis. (**E**) comparison of cell counts between CDK4/6^{high} and CDK4/6^{low}. ***$p < 0.001$. P-value is calculated by two-sided log rank test. (**F**) Bright-field images and cell viability of patient-derived organoids (PDOs) from CC-IV subtype treated with palbociclib. ***$p < 0.001$. Data are presented as mean ± standard deviation (SD). Statistical analysis was performed using two-way ANOVA followed by Benjamini-Hochberg corrected post-hoc tests. Scale bar, 200 µm. (**G**) half-maximal inhibitory concentration (IC50) of palbociclib in PDOs. ***$p < 0.001$. Data are presented as mean ± SD. Statistical analysis follows the criteria described in (**F**). (**H**) heatmap illustrating potential drug targets across the four subtypes, with each row representing a drug-targeting protein. The color gradient indicates the abundance of drug-targeting proteins. (**I**) differences in kinase activity of drug targets among four subtypes. Boxplot construction follows the criteria described in Fig. 1D. (***$p < 0.001$, **$p < 0.01$, *$p < 0.05$). (**J**) schematic summary of the characteristics of the four CC subtypes

of immunotherapy in CC (Figure. S9A-B) [10]. These molecules provided a biological basis for the synergistic effects of palbociclib and immune checkpoint inhibitors, especially in CC-IV.

Our findings established a proteome-based molecular classification of CC, which refined CC heterogeneity, TME characterization, and identified potential therapeutic targets for each subtype (Fig. 2J). We also conducted in-depth research on the therapeutic effect of palbociclib on CC-IV, highlighting its significant potential. A potential limitation of our study is the sample size. Future studies in large prospective cohorts are warranted to validate the proteomic subtypes and evaluate the efficacy of palbociclib in clinical trials.

Abbreviations

APC	Antigen-Presenting Cell
CC	Cervical cancer
DEP	Differentially Expressed Proteins
DNA	Deoxyribose Nucleic Acid
ECM	Extracellular matrix
EMT	Epithelial-Mesenchymal Transition
GSEA	Gene Set Enrichment Analysis
GSVA	Gene Set Variation Analysis
HLA	Human Leukocyte Antigen
MHC	Major Histocompatibility Complex
TIM	Tumor Immune Microenvironment
TF	Transcription Factors
TME	Tumor microenvironment

Supplementary information

The online version contains supplementary material available at https://doi.org/10.1186/s40364-026-00896-1.

Supplementary Material 1

Supplementary Material 2

Supplementary Material 3

Supplementary Material 4

Supplementary Material 5

Supplementary Material 6

Supplementary Material 7

Supplementary Material 8

Supplementary Material 9

Supplementary Material 10

Supplementary Material 11

Supplementary Material 12

Supplementary Material 13

Supplementary Material 14

Supplementary Material 15

Supplementary Material 16

Acknowledgements
Not applicable.

Author contributions
TY Yang and LP Guo collected the data and did the statistical analysis. DY Liu provided the samples. CB Li, LP Guo and TY Yang did the experiments and organized the manuscript. CB Li and KQ Hua revised the manuscript and guided the whole process.

Funding
This study was supported by Shanghai Science and Technology Commission (23Y11901600).

Data availability
All the data generated or analyzed during this study are included in this article and its supplementary information files were available from the author upon reasonable request.

Declarations

Ethics approval and consent to participate
This study was approved by the institutional ethics review board of Shanghai OB/GYN Hospital (number: 2022–143). Written informed consent was signed for all experiments involving patients.

Consent for publication
Not applicable

Competing interests
The authors declare no competing interests.

Received: 29 November 2025 / Accepted: 13 January 2026
Published online: 27 March 2026

References

1. Cohen PA, Jhingran A, Oaknin A, Denny L. Cervical cancer. Lancet. 2019;393(10167):169–82.
2. Cancer Genome Atlas Research Network. Integrated genomic and molecular characterization of cervical cancer. Nature. 2017;543(7645):378–84.
3. Cancer Genome Atlas Research N, et al. Integrated genomic and molecular characterization of cervical cancer. Nature. 2017;543:378–84.

4. Gao C, Zhou Q, Liu L, Liu H, Yang Y, Qu S, et al. Stratification by mutational landscape reveals differential immune infiltration and predicts the recurrence and clinical outcome of cervical cancer. Phenomics. 2025;5(4):384–403.
5. Yu J, Gui X, Zou Y, Liu Q, Yang Z, An J, et al. A proteogenomic analysis of cervical cancer reveals therapeutic and biological insights. Nat Commun. 2024;15(1):10114.
6. Xu M, Cao C, Wu P, Huang X, Ma D. Advances in cervical cancer: current insights and future directions. Cancer Commun (Lond). 2025;45(2):77–109.
7. Cao C, Xu Q, Zhu Z, Xu M, Wei Y, Lin S, et al. Three-dimensional chromatin analysis reveals Sp1 as a mediator to program and reprogram HPV-host epigenetic architecture in cervical cancer. Cancer Lett. 2024;588:216809.
8. Wishart DS, Feunang YD, Guo AC, Lo EJ, Marcu A, Grant JR, et al. DrugBank 5.0: a major update to the DrugBank database for 2018. Nucleic Acids Res. 46(D1):D1074–82.
9. Booth L, Roberts J, Poklepovic A, Dent P. The CHK1 inhibitor SRA737 synergizes with PARP1 inhibitors to kill carcinoma cells. Cancer Biol Ther. 2018;19(9):786–96.
10. Alrouji M, Alshammari MS, Anwar S, Venkatesan K, Shamsi A. Mechanistic roles of transcriptional cyclin-dependent kinases in Oncogenesis: implications for cancer therapy. Cancers (Basel). 2025;17(9):1554.

Publisher's Note